Journal of
Ceramic Science
and Technology

J. Ceram. Sci. Tech., **05** [03] 217-222 (2014)
DOI: 10.4416/JCST2014-00010
available online at: http://www.ceramic-science.com

Synthesis and Characterization of Nano-/Micro-Crystalline SnO using Microwave and Hydrothermal Techniques

A.M. EL-Rafei*[1], H. Youssef[1] and N. M. Ahmed[2]

[1]Refractories, Ceramics and Building Materials Dept., National Research Center, 12622 Dokki, Cairo, Egypt
[2]Photovoltaic Department, Electronic Research Institute (ERI), Dokki, Giza, Egypt

received March 12, 2014; received in revised form May 2, 2014; accepted June 6, 2014

Abstract

Microwave (M-H) and conventional hydrothermal (C-H) synthesis of nano-/micro-sized SnO are compared. The phase composition and morphology of the products were investigated by means of X-ray diffraction (XRD) and scanning electron microscopy (SEM), respectively. The XRD results of microwave-heated samples indicated early crystallization of tetragonal romarchite phase after only 1 h at 120 °C compared to 4 h at 120 °C for the conventional method. The crystallization path under microwave heating showed the presence of abhurite phase with an intermediate composition between tin oxide and the starting precursor. Also, romarchite (SnO) decomposes at 700 °C for 1 h in air and transforms into nano-sized cassiterite (SnO_2).

Keywords: Tin oxides, semiconductors, microwaves, nanostructures, chemical synthesis

I. Introduction

Tin oxides, such as tetragonal SnO and rutile-type SnO_2, have attracted a lot of attention as functional materials. SnO is used in P-type semiconductors, high-energy-density rechargeable lithium batteries [1] and solar energy storage [2]. SnO_2 is an n-type wide-band gap semiconductor (3.6 eV) used for various devices, such as coating materials [3], transparent conductive electrodes for solar cells and optical electronic devices [4], gas sensors [5–7], electrochromic devices [8] and photoelectrodes in dye-sensitized solar cells (DSSCs) [9–10]. The success of previous applications relies on the ability to obtain cost-effective and high-quality nano-sized materials with uniform grain structure. Sn_3O_4 is a non-stoichiometric structure that deserves attention, especially for the preparation of SnO_2 from SnO. The decomposition of SnO passes first through Sn_3O_4 and ends with the formation of SnO_2 and metallic tin [11–12].

SnO is a versatile intermediate to metallic Sn, Sn_3O_4, and SnO_2, however, the steady growth of SnO single-crystal is relatively difficult because Sn (II) is a thermodynamically unstable phase and is easily oxidized to Sn (IV) in air; hence its preparation is very challenging [13–15].

Different routes and methods have been developed to synthesize SnO and SnO_2 nanoparticles. These include high-energy ball milling, homogeneous precipitation, sonochemical, hydrothermal, solvothermal, microemulsion, sol-gel, spray pyrolysis, solid-state reaction-thermal oxidation, carbothermal reduction, rapid oxidation and microwave heating [5, 16–25]. Microwave heating is a promisingtechnique with rapidly increasing applications. Diverse microwave systems include household [26–32] or laboratory [33–34] instruments. In particular, when compared to the conventional-hydrothermal processes, microwave-assisted hydrothermal processes enhance powder crystallinity, increase the rate of formation and decrease the by-product; it also enhances material quality and size distribution. This method is considered to be green, produces higher temperature homogeneity, and is considerably faster than conventional heat sources. These advantages are even more evident when compared to the "ceramic route", where extended periods for grinding and firing solid precursors followed by annealing in controlled gas atmosphere are necessary.

Additionally, it offers further advantages, such as energy saving, simplicity and low cost; therefore, it has the potential of being used in large-scale commercial productions [35–41].

$SnCl_4{\cdot}5H_2O$ was found to be the common source for producing SnO_2 [26–27, 42–47] whereas $SnCl_2{\cdot}2H_2O$ is the main precursor whenever SnO is needed [28–32]. On the other hand, alkali solutions of NH_4OH, NaOH, KOH, and urea are the main mineralizers used in obtaining both II and IV phases of tin at different durations and temperatures [27, 33–34, 42]. Synthesized SnO powder is readily converted to SnO_2 when subjected to further calcination at temperatures ranging from 400 to 800 °C and reaction time of 1 to 5 h, depending on each specific method and instrument used [30–32 34].

This paper describes the preparation of nano- to micrometric SnO with the use of free surfactant conventional (C-H) and microwave hydrothermal conditions (M-H). Obviously, the products are compared with those prepared in other microwave conditions. Thermal decompo-

* Corresponding author: amira_elrafei@yahoo.com

sition of the prepared romarchite (SnO) at 700 °C, conducted in air atmosphere for 1 h was also studied.

II. Materials and Experimental Procedure

(1) Preparation

For the synthesis of tin oxide (SnO) under conventional and microwave hydrothermal conditions, a calculated amount of $SnCl_2{\cdot}2H_2O$ was dissolved in an appropriate amount of 1.0 M HCl solution, which was then transferred to a 250-ml volumetric flask to be homogenized (stock solution). For the synthesis of SnO under conventional-hydrothermal (C-H) conditions, 50 ml of the stock solution was loaded into a Teflon container of a handmade autoclave (100 ml capacity), with the addition of an appropriate amount of urea. After it had been sealed, the autoclave was treated for 4 h at 100 – 160 °C whereas, for the synthesis of SnO under microwave-hydrothermal (M-H) conditions, 20 ml of the stock solution and appropriate amount of urea were charged into the vessels of an accelerated reaction microwave system, CEM MARS 5 microwave extraction and digestion system, which work at different levels of energy ranging from 0 to 100 % of 1800 Watt power energy. All samples were treated at 100 to 120 °C for 0.5 to 4 h. After cooling, the powders were collected, washed several times in distilled water and then dried in an oven at 100 °C.

Calcination of the prepared SnO at 700 °C was conducted for 1 h in air and performed only on the sample prepared with conventional hydrothermal treatment for 4 h at 160 °C.

(2) Characterization

XRD analysis of the as-prepared powders was performed using BRUKUR D_8 ADVANCE with secondary monochromatic beam CuKα radiation at 40 Kv and 40 mA, whereas the microstructure of the as-prepared powders was examined using scanning electron microscopy (SEM), model Philips XL 30, with accelerating voltage 30 kV, magnification up to 400 000 x and resolution for W. 3.5 nm. Samples were coated with a thin film of gold prior to analysis.

III. Results and Discussion

(1) Phase composition of the as-prepared samples and calcined sample

Fig. 1 shows XRD patterns of the samples prepared with conventional heating (C-H) for 4 h at 100 – 160 °C. The data shows that samples prepared at 100 °C, which are beige in color, witnessed the first appearance of poorly indexed crystalline mixture of tin oxides which may be assigned mainly to orthorhombic SnO (PDF#77 – 2296) with minor peaks of other tin oxide phase; namely romarchite SnO (Fig. 1a). At 120 °C, the precipitate is very pale gray in color, a slight improvement occurs in the peak but still weak intensities, which refer to the peaks of romarchite SnO (PDF#78 – 1913) (Fig. 1b). The XRD pattern of the sample heated at 140 °C, which was pale gray in color, showed a romarchite SnO structure (PDF #78 – 1913) with sharp intensities. However, the intensities of the (001) and (002) peaks of SnO powder show higher intensity ratios than those of the standard diffraction pattern (Fig. 1c). This agrees well with certain findings [34 48]. According to Pires *et al.* [34], the natural tendency of the SnO nanoplates to align themselves parallel to the sample holder was responsible for the increase in the intensity of the (002) peaks in the X-ray diffractograms. As the temperature proceeds to 160 °C (Fig. 1d), the diffraction pattern implies strong and narrow peaks matching well with the tetragonal black romarchite (SnO) structure (PDF#78 – 1913).

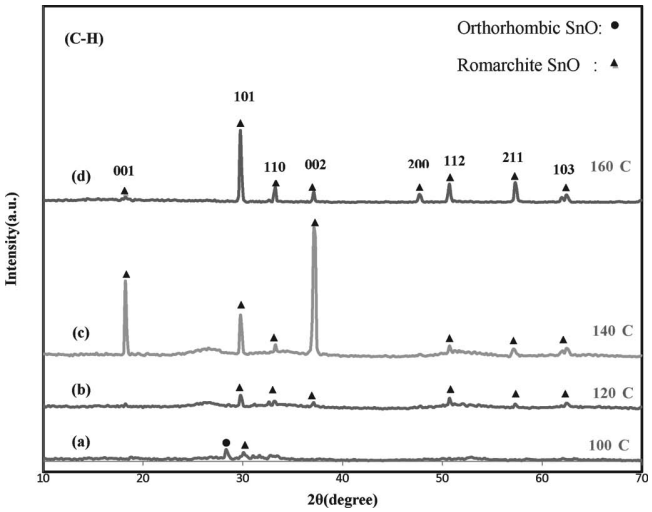

Fig. 1: XRD patterns of the C-H samples treated for 4 h at different temperatures: a) 100, b) 120, c) 140 and d) 160 °C.

Fig. 2 shows the XRD spectra of the as-prepared SnO under microwave irradiation at 100 to 120 °C for different durations (30 min to 4 h). According to Fig. 2a, the main peaks of the XRD data for samples heated for 4 h at 100 °C, their color being grayish beige, indicate the co-presence of abhurite ($Sn_{21}Cl_{16}(OH)_{14}O_6$) with hexagonal symmetry (PDF #72 – 0252) as the main developing phase, along with some peaks of lower intensities belonging to tetragonal romarchite SnO. Samples heated for 30 min at 120 °C, which are beige in color, indicated the domination of abhurite peaks with no signs of any other phases (Fig. 2b).

On heating for 1 h at 120 °C, strong narrow peaks of tetragonal black romarchite prevail as the sole phase present in the synthetic powder (Fig. 2c). Under such microwave conditions, a further increase in the treatment time to 4 h positively affects the intensities and sharpness of the romarchite peaks (Fig. 2d), it has no effect on the oxidation state of the SnO at this temperature.

After heat treatment in air for 1 h at 700 °C, samples obtained at 160 °C/4 h with the conventional hydrothermal process were completely oxidized to SnO_2 as a single phase and their XRD lines match perfectly the typical tetragonal cassiterite (PDF#41 – 1445) [49],as shown in Fig. 3.

(2) Microstructure analysis

Figs. 4 (A and B) describe the different morphologies of the as-prepared products prepared for different durations at 100 to 160 °C under both conventional and microwave heating, respectively. Fig. $4A_1$ shows the micrograph of the sample obtained at 100 °C/4 h under conventional heating presenting the first stage of SnO crystallization process in which particles of indistinct shape and wide

size range could be observed. Meanwhile, the microwave samples heated for only 30 min at 100 °C show uniformly sized nano-particles of spherical morphology in a homogenous texture with a narrow range of particle size distribution from 10 to 15 nm (Fig. 5a). When the treatment time is increased to 4 h (Fig. $4B_1$), the powder shows various crystalline aggregates (thread balls-like) of non-separated platelets (identified by means of XRD as abhurite in Fig. 2a along with some minor SnO structures) consisting of stacked platelets of hexagonal morphology (identified as SnO in Fig. 2a). Elevating the microwave temperature to 120 °C (for 30 min) caused a notable change in the abhurite aggregates towards thinner and more developed six-sided platy to tabular abhurite crystals with a particle size in the range of 500 nm – 0.2 μm in thickness and less than 20 μm in width (Fig. $4B_{2)}$. In Fig. $4B_3$, a clear improvement in the crystallization process could be seen when the time was increased to 1 h at 120 °C where well developed SnO crystals of decahedral romarchite symmetry are dominant all over the scanned area, matching the results of the XRD data shown in Fig. 2c.

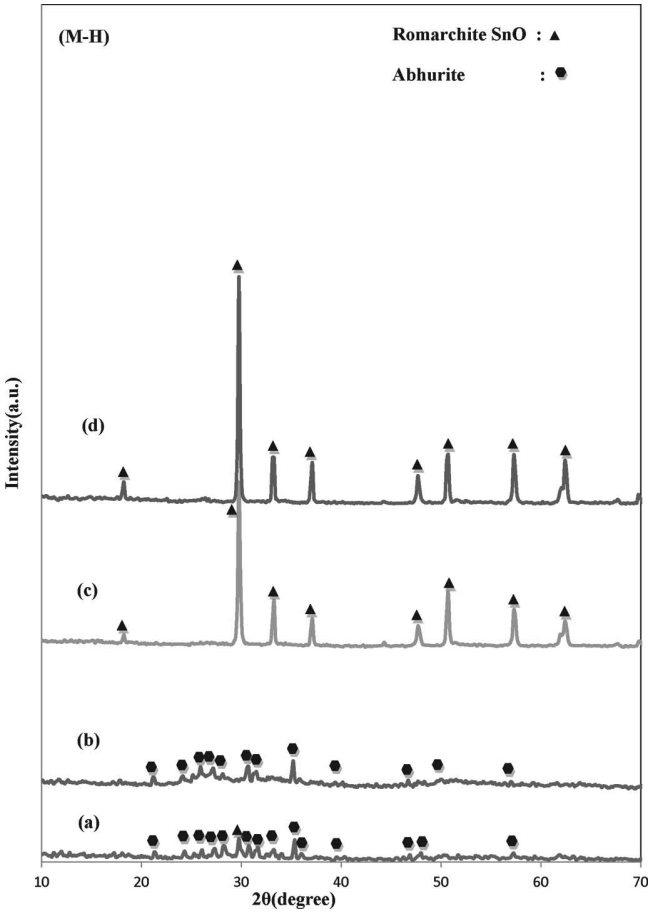

Fig. 2: XRD patterns of the M-H heated samples at different temperatures and durations: a) 100 °C/4 h, b) 120 °C/30 min, c) 120 °C/1 h and d) 120 °C/4 h.

The increase in the treatment time to 4 h at 120 °C strongly affects the powder crystallinity as shown in Fig. $4B_4$, in which bigger crystals of romarchite of less than 10 – 50 μm in size are seen. On the other hand, the micrographs of C-H samples, obtained after long duration of 4 h at temperatures of 120 and 140 °C still show spherical nano-particles in the size range from 85 to < 200 nm (Fig. $4A_2$ and A_3). At 160 °C, different sizes of square-like (faceted) grain crystalline structure of tetragonal romarchite are obtained as indicated in Fig. $4A_4$.

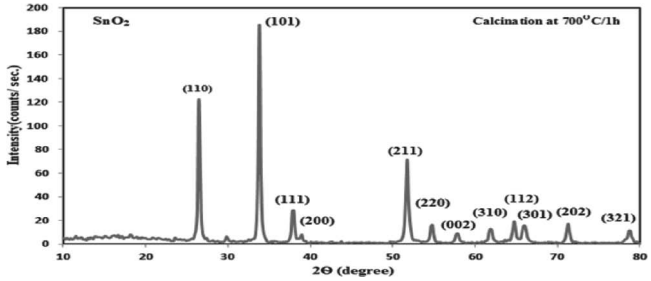

Fig. 3: XRD pattern of SnO_2 obtained after product calcination at 700 °C for 1 h.

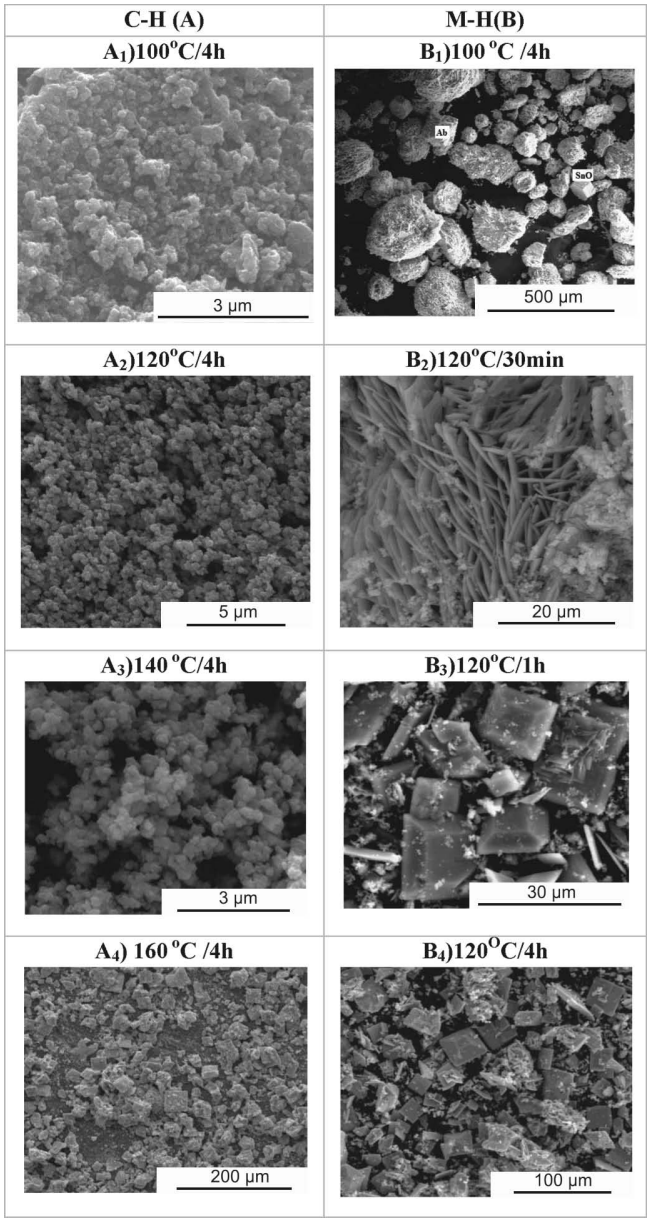

Fig. 4: SEM images of tin oxide powders obtained at different temperatures and durations under both conventional and microwave heating. Ab: refers to Abhurite in B_1.

After calcination for 1 h at 700 °C of the sample treated in the conventional hydrothermal process at 160 °C/4 h, romarchite (SnO) decomposes and transforms into nano-

cassiterite SnO_2 in the form of spherical-shaped particles with sizes in the range of 20 to 70 nm as shown in Fig. 5b.

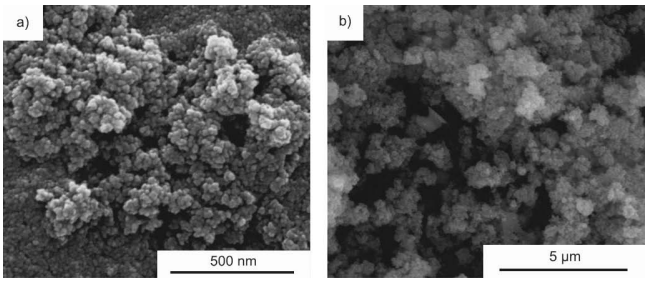

Fig. 5: Uniform nano-particles developed under microwave heating a) at 100 °C/30 min and b) nano-particles of cassiterite, SnO_2, obtained after calcination of romarchite at 700 °C/1 h.

XRD results of microwave-heated samples clearly indicate early crystallization of the tetragonal romarchite phase after only 1 h at 120 °C as compared with 4 h at 120 °C for the C-H method. Pires *et al.* [34], who used the same version of our microwave instrument and precursor but different mineralizers (NaOH, KOH and NH_4OH), reported the formation of SnO at 120 °C or 180 °C for 2 or 6 h and they treated SnO for 2 h at 800 °C to prepare SnO_2.

However, for the major applications of romarchite SnO in lithium battery anodes, coating materials and catalysts in maleamic acid cyclization, and lactic acid polymerization, synthesis of romarchite SnO has not been as widely studied as the synthesis of cassiterite owing to its instability. In this work, based on application the microwave-hydrothermal technique, we have succeeded in preparing SnO at a lower temperature and shorter time in comparison with other findings [34].

One of the methods to improve the densification behavior of SnO_2 is based on the preparation of homogeneous nano-sized powders, which are a key driving force for densification. So the obtained nano-SnO_2 powder may be sintered with additions of other additives such as In_2O_3 in order to fabricate ITO ceramics for use as targets for the sputtering technique to prepare ITO thin films when highly conductive, transparent thin films are required for flat panel displays, defrosting windows, electromagnetic shielding and solar cells, etc. This work may be continued in further research.

IV. Interpretation of the Results

The obtained results could be explained based on the microwave heating process, which fundamentally differs from the conventional process in that heat is initiated as a result of interaction between the dielectric properties of the materials and the oscillating electromagnetic field generated by the microwaves. This leads to the rotation of molecular dipoles and causes subsequent energy dissipation as heat from the internal resistance to that rotation [50]. Therefore, the heating in this process is volumetric and penetrating and distributed in a fast and homogenous way, causing the reactants to be set in action at the same time and favoring earlier and simultaneous nucleation [51–52]. In contrast, the presence of different generations of crystals is a characteristic property of conventional heating technique, where the co-presence of differently sized crystals in the same product is attributed to the slow temperature rise allowing the nucleation to continue for nearly the entire duration of the process [53].

J. Jouhannaud *et al.* [47] used tin tetrachloride as precursor for SnO_2 synthesis with microwave heating. They reported that the generation of tin (IV) oxide nanoparticulate is based on microwave thermohydrolysis of metal salt solutions [54–56]. This could be viewed in the light of knowing that most polyvalent cations are readily hydrolyzed and that deprotonation of coordinated water molecules is greatly accelerated with increasing temperature. The produced hydrolyzed species are intermediates to precipitation of metal oxides. Based on the above, Pires *et al.* [34] explains the formation of nanoparticles as starting with the hydrolysis of the $SnCl_2{\cdot}2H_2O$ precursor in aqueous solution to produce $Sn(OH)_2$, leading to the formation of SnO nanoplates according to the following possible chemical reaction:

$$Sn(OH)_2 \downarrow \rightarrow Sn^{2+} + 2\,OH^- \quad (1)$$

$$Sn(OH)_2 \leftrightarrow SnO + H_2O \uparrow \quad (2)$$

In the present work, the previous reaction path seems to be applicable only for the conventionally heated samples. However, XRD and SEM results of microwave samples indicated the presence of abhurite ($Sn_{21}Cl_{16}(OH)_{14}O_6$) structure as the major phase obtained after heating at 100 °C/4 h and, at 120 °C/30 min. Abhurite converts readily to tetragonal romarchite on a slight increase in the treatment time from 30 min to 1 h at the 120 °C. Thus, the later finding probably suggests the introduction of abhurite as an additional step in the hydrolysis process encountered in the crystallization passage of SnO synthesis under microwave conditions. The following path may be suggested:

$$Sn_{21}Cl_{16}(OH)_{14}O_6 + 6H_2O \rightarrow 21Sn^{2+} + 16Cl^- + 26OH^- \quad (3)$$

$$21\,SnO + 15H_2O + Cl^-_{16} \rightarrow Sn_{21}Cl_{16}(OH)_{14}O_6 + 16OH^- \quad (4)$$

Natural abhurite has a tin hydroxychloride composition of $Sn_{21}Cl_{16}(OH)_{14}O_6$ stoichiometric compositionand a thin, six-sided, platy to tabular crystal structure with trigonal symmetry. Its formation is confined to the reaction of pure tin with sea water and has been exclusively associated with tin ingots from shipwrecks [57–58].

V. Conclusions

In this work, we report for the first time on the preparation of abhurite phase with the microwave-hydrothermal technique, which may be adapted to specific applications. Microwave and conventional hydrothermal synthesis of micro-/nano-sized SnO is compared. Products of both methods yielded different morphologies, i.e. mainly square-like and decahedral. The powders produced with microwave heating showed earlier crystallization of the tetragonal romarchite phase after only 1 h at 120 °C compared with 4 h at 120 °C for the conventional method. The crystallization path of microwave-heated samples witnessed the formation of abhurite as an intermediate composition in the reaction passage usually encountered

in SnO preparation. This confirms the formation of abhurite with the microwave technique, which may contribute to understanding the reaction mechanism that usually occurs between tin (II) chloride and urea to obtain tin oxide. The abhurite structure withstood conditions up to 120 °C/30 min after which a slight increase in the treatment time resulted in fast conversion to tetragonal romarchite with good crystallinity. The calcination of romarchite (SnO) powder for 1 h at 700 °C in air readily converts it to nano-sized SnO_2 with a cassiterite tetragonal structure.

References

1 Li, H., Huang, X., Chen, L.: Structure and electrochemical properties of anodes consisting of modified SnO, *J. Power Sources*, **81 – 82**, 335 – 339, (1999).

2 Ferrere, S., Zaban, A., Gregg, B.A.: Dye sensitization of nanocrystalline tin oxides by perylene derivatives, *J. Phys. Chem. B*, **101**, 4490 – 4493, (1997).

3 Zhang, J., Gao, L.: Synthesis and characterization of nanocrystalline tin oxide by sol-gel method, *J. Solid State Chem.*, **177**, 1425 – 1430, (2004).

4 Beyer, W., Hüpkes, J., Stiebig, H.: Transparent conducting oxide films for thin film silicon photovoltaics, *Thin Solid Films*, **516**, 147 – 154, (2007).

5 Rella, R., Serra, A., Siciliano, P., Vasanelli, L., De, G., Licciulli, A.: CO sensing properties of SnO_2 thin films prepared by the sol-gel process, *Thin Solid Films*, **304**, 339 – 343, (1997).

6 Nayral, C., Ould-Ely, T., Maisonnat, A. *et al.*: A novel mechanism for the synthesis of tin/tin oxide nanoparticles of low size dispersion of nanostructured SnO_2 for the sensitive layers of gas sensors, *J. Adv. Mater.*, **1**, 61 – 63, (1999).

7 Leite, E.R., Weber, I.T., Longo, E., Varela, J.A.: A new method to control particle size and particle size distribution of SnO_2 nanoparticles for gas sensor applications, *J. Adv. Mater.*, **12**, [13], 965 – 968, (2000).

8 Pawlicka, A.: Development of Electrochromic Devices. *Recent Patents on Nanotechnology*, **3**, 177 – 181, (2009).

9 Lee, J.H., Park, N.G., Shin, Y.J.: Nano-grain: SnO_2 electrodes for high conversion efficiency SnO_2-DSSC, *J. Sol. Energy Mater. Sol. Cell*, **95**, 179 – 183, (2011).

10 Yasuhiro, T., Hara, K., Takano, S., Sayama, K., Arakawa, H.: Investigations on anodic photocurrent loss processes in dye sensitized solar cells, comparison between nanocrystalline SnO_2 and TiO_2 films, *J. Chem. Phys. Lett.*, **364**, 297 – 302, (2002).

11 Lawson, F.: Tin oxide – Sn_3O_4, *Nature London*, **215**, 955 – 956, (1967).

12 Cahen, S., David, N., Fiorani, J.M., Vilas, I.M.: Thermodynamic modelling of the O-Sn system, *Thermochim. Acta.*, **403**, 275 – 285, (2003).

13 Dai, Z.R., Pan, Z.W., Wang, Z.L.: Growth and structure evolution of novel tin oxide diskettes, *J. Am. Chem. Soc.,* **124**, 8673 – 8680, (2002).

14 Wang, Z.L., Pan, Z.W.: Junctions and networks of SnO nanoribbons, *J. Adv. Mater.*, **14**, [15], 1029 – 1032, (2002).

15 Jia, Z., Zhu, L., Liao, G., Yu, Y., Tang, Y.: Preparation and characterization of SnO nanowhiskers, *Solid State Commun.*, **132**, 79 – 82, (2004).

16 Xia, L., Yang, B., Fu, Z., Yang, Y., Yan, H., Xu, Y., Fu, S., Li, G.: High-yield solvothermal synthesis of single-crystalline tin oxide tetragonal prism nanorods, *J. Mater. Lett.*, **6**, 1214 – 1217, (2007).

17 Acarbas, O., Suvacı, E., Dogan, A.: Preparation of nano-sized tin oxide (SnO_2) powder by homogeneous precipitation, *Ceram. Int.*, **33**, [4], 537 – 542, (2007).

18 Patil, G.E., Kajale, D.D., Gaikwad, V.B., Jain, G.H.: Spray pyrolysis deposition of nanostructured tin oxide thin films, *J. Inter. Sch. Res. Net. ISRN Nanotechnology,* Article ID 275872, 1 – 5, (2012).

19 Song, K.C., Kim, J.H.J.: Synthesis of high surface area tin oxide powders via water-in-oil microemulsions, *Powder Technol.,* **107**, 268 – 272, (2000).

20 Sedghi, S.M., Mortazavi, Y., Khodadadi, A., Sahraei, O.A., Naseh, M.V.: Sonochemically prepared SnO_2 quantum dots as a selective and low temperature CO sensor, *Intern. J. Chem. and Biol. Eng.,* **2**, [2], 69 – 73, (2009).

21 Kersen, U., Holappa, L.: H_2S-sensing properties of SnO_2 produced by ball milling and different chemical reactions, *Anal. Chim. Acta,* **562**, 110 – 114, (2006).

22 Chen, Y., Zhu, J., Zhu, X., Ma, G., Liu, Z., Min, N.: Gas sensing property and microstructure of SnO_2 nanocrystalline prepared by solid state reaction/thermal oxidation, *J. Mater. Sci. and Eng. B*, **99**, 52 – 55, (2003).

23 Sedghia, M.S., Mortazavib, Y., Khodadadi, A.: Low temperature CO and CH_4 dual selective gas sensor using SnO_2 quantum dots prepared by sonochemical method, *Sensor. Actuat., B-Chem.*, **145**, 7 – 12, (2010).

24 Thanasanvorakun, S., Mangkorntong, P., Choopun, S., Mangkorntong, N.: Characterization of SnO_2 nanowires synthesized from SnO by carbothermal reduction process, *Ceram. Int.*, **34**, 1127 – 1130, (2008).

25 Ma, X.L., Li, Y., Zhu, Y.L.: Growth mode of the SnO_2 nanobelts synthesized by rapid oxidation*, Chem. Phys. Lett.*, **376**, 794 – 798, (2003).

26 Cirera, A., Vilà, A., Cornet, A., Morante, J.R.: Properties of nanocrystalline SnO obtained by means of microwave process, *Mat. Sci. Eng. C*, **15**, 203 – 205, (2001).

27 Srivastava, A., Lakshmikumar, S.T., Srivastava, A.K., Rashmi, Jain, K.: Gas sensing properties of nanocrystalline SnO_2 prepared in solvent media using a microwave assisted technique, *Sensor. Actuat. B*, **126**, 583 – 587, (2007).

28 Wu, D-S., Han, C.-Y., Wang, S.-Y., Wu, N.-L., Rusakova, I.-A.: Microwave-assisted solution synthesis of SnO nanocrystallites, *Mater. Lett,* **53**, 155 – 159, (2002).

29 Krishnakumar, T., Pinna, N., Kumari, K.P., Perumal, K., Jayaprakash, R.: Microwave-assisted synthesis and characterization of tin oxide nanoparticles, *Mater. Lett.,* **62**, 3437 – 3440, (2008).

30 Parthibavarman, M., Hariharan, V., Sekar, C.: High-sensitivity humidity sensor based on SnO_2 nanoparticles synthesized by microwave irradiation method, *Mater. Sci. and Eng. C*, **31**, 840 – 844, (2011).

31 Parimala, S.S., Selin, C., Gnanamani, A., Mandal, A.B.: Synthesis and characterization of nano crystalline tin (IV) oxide from tin (II) chloride using combined microwave traditional calcinations procedures, *Current Res. in Chemistry*, **4**, (3), 60 – 67, (2012).

32 Singh, A.K., Nakate, U.T.: Microwave synthesis, characterization and photocatalytic properties of SnO_2 nanoparticles, *Advances in Nanoparticles*, **2**, 66 – 70, (2013).

33 Krishna, M., Komarneni, S.: Conventional- vs microwave-hydrothermal synthesis of tin oxide, SnO_2 nanoparticles, *Ceram. Int.*, **35**, 3375 – 3379, (2009).

34 Pires, F.I., Joanni, E., Savu, R., Zaghete, M.A., Longo, E., Varela, J.A.: Microwave-assisted hydrothermal synthesis of nanocrystalline SnO powders, *Mater. Lett.,* **62**, 239 – 242, (2008).

35 Rizzuti A., Leonelli C.: Microwave advantages in inorganic synthesis of $La_{0.5}Sr_{0.5}MnO_3$ powders for perovskite ceramics, *Proces. and App. of Ceram.*, **3**, [1 – 2], (2009).

[36] Yuan, Cao, Y., Wei, H.-J., Xia, Z.-N.: Advances in microwave assisted synthesis of ordered mesoporous materials, *T. Nonferr. Metal. Soc.*, **19**, 656 – 664, (2009).

[37] Phuruangra, A., Thongtem, S., Thongtem, T.: Microwave hydrothermal synthesis and characterization of copper sulfide with different morphologies, *Chalcogenide Lett.*, **10**, [10], 359 – 365, (2013).

[38] Kharisov, B.I., Kharissova, O.V., Méndez, U.O.: Microwave hydrothermal and solvothermal processing of materials and compounds, (Chapter 5), The development and application of microwave heating edited by Wenbin Cao, ISBN 978 953 51 0835 1, 212 pages, Publisher: InTech, Chapters published November 07, 2012 under CC BY 3.0 license DOI: 10.5772/2619, 107 – 140, (2012).

[39] Wu, S.-S., Jia, Q., Sun, Y.-L., Shan, S.-Y., Jang, L.-H., Wang, Y.-M.: Microwave hydrothermal preparation of flower-like ZnO microstructure and its photocatalytic activity, *T. Nonferr. Metal. Soc.*, **22**, 2465 – 2470, (2012).

[40] Qi, H., Huang, J.-F., Cao, L.-Y., Wu, J.-P., Wang, D.-Q.: One-dimensional CuS microstructures prepared by a PVP-assisted microwave hydrothermal method, *Ceram. Int.*, **38**, 2195 – 2200, (2012).

[41] Ortiz-Landeros, J., Gómez-Yáñez, C., López-Juárez, R., Dávalos-Velasco, I., Pfeiffer, H.: Synthesis of advanced ceramics by hydrothermal crystallization and modified related methods, *J. Adv. Ceram.*, **1**, [3], 204 – 220, (2012).

[42] Zhu, J-J., Zhu, J-M., Liao, X-H., Fang, J-L., Zhou, M-G., Chen, H-Y.: Rapid synthesis of nanocrystalline SnO powders by microwave heating method, *Mater. Lett*., **53**, 12 – 19, (2002).

[43] Du, F., Guo, Z., Li, G.: Hydrothermal synthesis of SnO_2 hollow microspheres, *Mater. Lett.*, **59**, 2563 – 2565, (2005).

[44] Paraguay-Delgado, F., Antunez-Flores, W., Miki-Yoshida, M., Aguilar-Elguezabal, A., Santiago, P., Diaz, R., Ascencio, J.A. : Structural analysis and growing mechanisms for long SnO_2 nanorods synthesized by spray pyrolysis, *Nanotechnology*, **16**, [6], 688 – 694, (2005).

[45] Chen, Z.W., Lai, J.K.L., Shek, C.H.: Bulk-quantity SnO_2 nanorods synthesized from simple calcining process based on annealing precursor powders, *J. Non-Cryst. Solids*, **351**, 3619 – 3623, (2005).

[46] Naoto, S., Atsushi, H., Shuuichi, A., Akio, F., Sakka, Y.: Assembly of hydrothermally synthesized tin oxide nanocrystals, *J. Vac. Sci. Technol. A*, **23**, 731 – 736, (2005).

[47] Jouhannaud, J., Rossignol, J., Stuerga, D.: Rapid synthesis of tin (IV) oxide nanoparticles by microwave induced thermohydrolysis, *J. Solid State Chem.*, **181**, 1439 – 1444, (2008).

[48] Wang, S.-C., Chiang, R.-K., Hua, P.-J.: Morphological and phase control of tin oxide single-crystals synthesized by dissolution and recrystallization of bulk SnO powders, *J. Eur. Ceram. Soc.*, **31**, 2447 – 2451, (2011).

[49] Yang, H., Hu, Y., Tang, A., Jin, S., Qiu, G.: Synthesis of tin oxide nanoparticles by mechanochemical reaction, *J. Alloy. Compd.*, **363**, 271 – 274, (2004).

[50] Kingston, H.M., Haswell, S.J.: Microwave-enhanced chemistry. *ACS.* Washington, DC, (1997).

[51] Rao, K.J., Vaidhyanathan, B., Ganguli, M., Ramakrishnan, P.A.: Synthesis of inorganic solids using microwaves, *Chem. Mater*., **11**, 882 – 895, (1999).

[52] Occelli, M.L., Robson, H.E.: Synthesis of microporous materials, Van Nostrand Reinhold, New York, **1**, 507, (1992).

[53] Bonaccorsi, L., Proverbio, E.: Influence of process parameters in microwave continuous synthesis of zeolite LTA, *Micropor. Mesopor. Mat.*, **112,** 481 – 493, (2008).

[54] Ondruschka, B., Bonrath, W., Stuerga, D.: Microwave in organic synthesis. Wiley, ISBN 3527314520, (2006).

[55] Bellon, K., Chaumont, D., Stuerga, D.: Flash synthesis of zirconia nanoparticles by microwave forced hydrolysis, *J. Mater. Res.*, **16**, 2619 – 2622, (2001).

[56] Caillot, T., Aymes, D., Stuerga, D., Viart, N., Pourrov, G.: Microwave flash synthesis of iron and magnetite particles by disproportionation of ferrous alcoholic solutions, *J. Mater. Sci.*, **37**, 5153 – 5158, (2002).

[57] http://www.mindat.org/mindat.org/min-4.html

[58] Edwards, R., Gillard, R.D., Williams, P.A.: The stabilities of secondary tin minerals: abhurite and its relationships to Sn(II) and Sn(IV) oxides and oxyhydroxides, *Mineral. Mag.*, **56**, 221 – 226, (1992).